Available online at www.sciencedirect.com
ScienceDirect
International Journal of Heat and Mass Transfer 51 (2008) 2676–2685
International Journal of HEAT and MASS TRANSFER
www.elsevier.com/locate/ijhmt

Spatial variation of heat flux at the metal–mold interface due to mold filling effects in gravity die-casting

S. Arunkumar, K.V. Sreenivas Rao, T.S. Prasanna Kumar *

Department of Metallurgical and Materials Engineering, Indian Institute of Technology Madras, Chennai 600036, India

Received 15 May 2007; received in revised form 17 September 2007
Available online 31 December 2007

Abstract

Most of the research work pertaining to metal–mold heat transfer in casting solidification either assumes no spatial variation in the air gap formation or limits the study to only those experimental systems in which air gap formation is uniform. However, in gravity die-casting, filling effects induce variation in thermal field in the mold and casting regions. In this paper, we show that this thermal field variation greatly influences the time of air gap initiation along a vertical mold wall, which subsequently leads to the spatial variation of air gap and in turn, the heat flux at the metal–mold interface.

In order to study the spatial variation of heat flux at the metal–mold interface, an experimental setup that involved mold filling was devised. A Serial-IHCP (inverse heat conduction problem) algorithm was used to estimate the multiple heat flux transients along the metal–mold interface. The analysis indicates that the fluxes at different mold segments (bottom, middle, and top) of the metal–mold interface reaches the peak value at different time steps, which shows that the initiation of air gap differs along the mold wall. The experimental and numerical results show that the heat transfer in the mold is two-dimensional during the entire period of phase change, which is initially caused by the filling effects and further enhanced by the spatial variation of the air gap at the metal–mold interface.

Keywords: Metal–mold heat transfer; Interface heat flux distribution; Inverse method; Mold filling transients; Air gap formation

1. Introduction

In gravity die-casting, rate of solidification is influenced by the heat flow from the metal to the mold. Unlike in pressure die-casting in which the mold and the metal are in perfect contact, in gravity die-casting the progressive development of air gap separates the metal surface from the mold wall. The spatial variation of the air gap is not only induced by the geometrical factors of the mold wall but also due to mold filling effects. This temporally and spatially varying air gap introduces an additional resistance to the heat flow from the metal to the mold. This thermal resistance has a considerable influence in the rate of solidification and thus affects the microstructure formation. Hence, it is important to understand the mechanism of heat transfer at the metal–mold interface to optimize the casting process.

Much effort has been devoted to understand the mechanism of heat transfer and to quantify the heat flux at the metal–mold interface [1–9]. More recently, Trovant and Argyropoulos [10,11] devised a coupling strategy to develop a correlation between the casting process parameters, such as roughness of the mold, air gap size and conductivity of the gas in the air gap. Carlos et al. [12] quantified the heat transfer coefficient at the metal–mold interface for various compositions of Al–Cu and Sn–Pb alloys. They expressed the heat transfer coefficient as a power function of time for various alloy compositions. Loulou et al. [13,14] devised an experimental setup to study and quantify the thermal contact resistance during the initial stages of solidification. They claim that the thermal contact resistance changes in a stepwise manner during the initial stages of solidification. Prabhu and Suresha

* Corresponding author.
E-mail address: tsp@iitm.ac.in (T.S. Prasanna Kumar).

0017-9310/$ - see front matter © 2007 Elsevier Ltd. All rights reserved.
doi:10.1016/j.ijheatmasstransfer.2007.10.020

Nomenclature

c	specific heat (J/kg K)	Y	measured temperature (K)
h	heat transfer coefficient (W/m^2 K)	x,y	coordinate directions (m)
q	heat flux (W/m^2)		
t	time (s)	*Greek symbols*	
T	computed temperature (K)	ϕ	sensitivity coefficient (km^2/W)
$\widehat{T}$	temperature computed for a few future time steps (K)	λ	thermal conductivity (W/m K)
		ρ	density (kg/m^3)
$\widehat{T}^+$	$\widehat{T}$ with enhanced heat flux at the elected segment (K)		

[15] studied the effect of superheat and mold and casting materials on the heat transfer at the metal–mold interface. Hallam and Griffiths [16] studied the air gap formation and its effect on heat transfer at the metal–mold interface in low-pressure and gravity die-castings of Al alloys. They quantified the heat transfer coefficient by measuring the coating thickness and the gap size.

Air gap formation and its temporal nature are evident from the above-mentioned work. However, the spatial variation of air gap and its effect on heat-flux has not been studied in detail. Authors in [17] estimated the spatially varying heat flux transients using a Serial-IHCP-algorithm at the metal–mold interface. They quantified the spatial variation of heat flux in rectangular plate castings. However, their analysis was restricted only to study the effect of geometrical factors on spatial variation of heat flux. The present work accounts for the mold filling effects also in order to analyze the spatial variation of both air gap formation and heat flux.

There are two major methods available in the literature for estimating boundary conditions at the metal–mold interface. In one of the methods [16,18], the interface heat transfer coefficient is calculated by measuring the size of the air gap at various time steps and by obtaining the corresponding thermal conductivity of the air/gas mixture formed in these gaps. This method can be used only if the heat flow at the metal–mold interface is unidirectional. Further, obtaining thermal conductivity of the air/gas mixture is very difficult. In another method [19], temperatures measured at the mold and the casting regions were used to calculate the heat flux transients using inverse heat conduction algorithms at the mold wall. These heat flux transients were then used to estimate the heat transfer coefficient at the interface.

The measurement of interface heat transfer coefficient was often done by careful design of experiments to induce one dimensional heat transfer. However, in practical situations of metal castings the metal–mold heat transfer is far more complicated due to complex casting geometry and filling transients. Hence, the use of heat transfer coefficient obtained from simplified experiments for multi-dimensional simulation of complex castings become highly questionable. In this paper, we have made an attempt to bring in the effect of mold filling transients on the formation of air gap along the vertical wall of the permanent mold.

The estimation of multiple heat fluxes at the metal–mold interface from the measured temperatures is described in [17]. The basic principle used in this technique is to estimate multiple heat flux components at the surface of the mold wall from the temperatures obtained at the interior points. Several algorithms [20,21] have been proposed to solve inverse heat conduction problems (IHCP). However the limitation of these algorithms is that the solution depends on the number of internal temperature measurements. Prasanna Kumar [22] developed a serial solution for the IHCP for multiple heat flux components at the unknown boundary. This Serial-IHCP-algorithm is capable of delineating multiple heat fluxes with over-specified as well as under-specified internal temperature measurements.

The main aim of this paper is to show the effects of filling transients on the initiation of air gap formation and how it leads to the spatial variation of heat flux at the metal–mold interface. The Serial-IHCP-algorithm [22] was used to estimate the multiple heat flux components along the metal–mold interface. The temperature measurements necessary for IHCP were obtained from the casting experiment that involved filling along a vertical mold wall.

2. Experimental setup

The objective of this work is to study the spatial and temporal variation of heat flux at the metal–mold interface during the air gap formation and to analyze the heat transfer in the mold wall due to filling. In order to accomplish this task, an experimental setup was devised as shown in Fig. 1a. The mold cavity consisted of two cast iron chills placed 60 mm apart and an insulating material placed on top, bottom and extreme ends of the cavity. Higher thickness (90 mm) and very low thermal conductivity (0.1 W/mK) of insulating walls are sufficient enough to assume those boundaries as adiabatic in the numerical modeling. Medium resistance mold coating was applied along the inner surfaces of the insulating walls to reduce the surface roughness. A sprue and a riser were placed on top of the

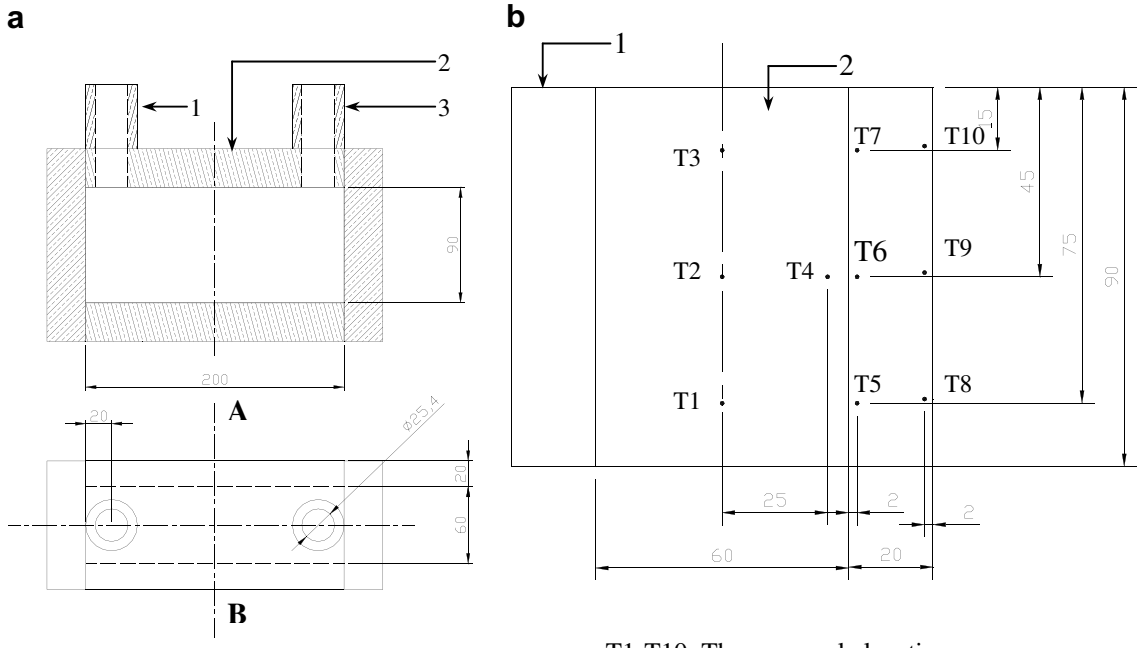

Fig. 1. (a) Sectional view and top view of the mold cavity and (b) section of casting and mold wall along A–B.

mold as shown in Fig. 1a. The thermocouple locations in the mold wall and inside the casing are shown in Fig. 1b.

The temperatures measured using the thermocouples were used to estimate heat fluxes using IHCP. Since the IHCP solution is highly sensitive to the temperature measurements, proper care was taken in the selection and fixing of thermocouples. The K-type thermocouples used in the experiment were mineral (MgO) insulated and covered with stainless steel sheath. The diameter of the thermocouple wires was 0.233 mm and that of the stainless steel sheath was 1 mm. The thermocouples were fixed in the mold wall through 1 mm holes to obtain snug fit and loaded by spring to ensure proper contact between the sensor tip and the mold wall. The spring-loaded thermocouples thus ensured positive contact throughout the experiment and the development of air envelope at the sensor tip was most unlikely even during the expansion of the mold wall. Since, the wire diameter of the thermocouples was minimal and having positive contact with the mold wall, the response lag in the temperature measurements in this experiment was insignificant.

The thermocouples were calibrated at the melting point of pure tin and found to have 0.5% error. Six thermocouples (three nearer to the inner surface of the mold wall and three on the outer surface of the mold wall) were placed in the mold to obtain the thermal histories to be used as inputs for IHCP. They were connected to the data acquisition system, which consisted of an Agilent 34970A data acquisition/switch unit and a computer.

Commercially available aluminum of 99.9% purity was melted in an induction furnace till the molten metal temperature reaches 750 °C. Then the molten metal was poured into the mold cavity through the sprue, in such a manner that filling process resembled bottom filling. Pouring was stopped once the metal reached the top of the riser placed on the other end of the cavity. Temperature recordings were started well before the metal was poured into mold cavity.

3. Mathematical modeling

Air gap formation in the metal–mold interface is a common phenomenon in gravity die-castings. The resistance induced by the air gap affects the heat flow from the metal to the mold to a large extent if the mold is metallic. Quantifying the heat flux at the metal–mold interface is not straight forward as the gap formation is not only irregular but also transient in nature. The 1-D IHCP algorithm which is generally employed for estimating the metal–mold interface heat flux is not appropriate in the case of gravity die-casting. Therefore, the Serial-IHCP-algorithm developed by Prasanna Kumar [22] and applied to bar and plate aluminum alloy castings [17] is adopted in this work to delineate the multiple heat fluxes at the metal–mold interface. The Serial-IHCP-algorithm is capable of computing independent heat fluxes in a serial manner as opposed to the simultaneous estimation. The algorithm is briefly explained here and the complete mathematical and implementation details can be found elsewhere [22].

The two dimensional section of the casting and mold wall is given in Fig. 1b. Since the mold cavity is symmetric along the vertical mid-plane and insulated on top and bot-

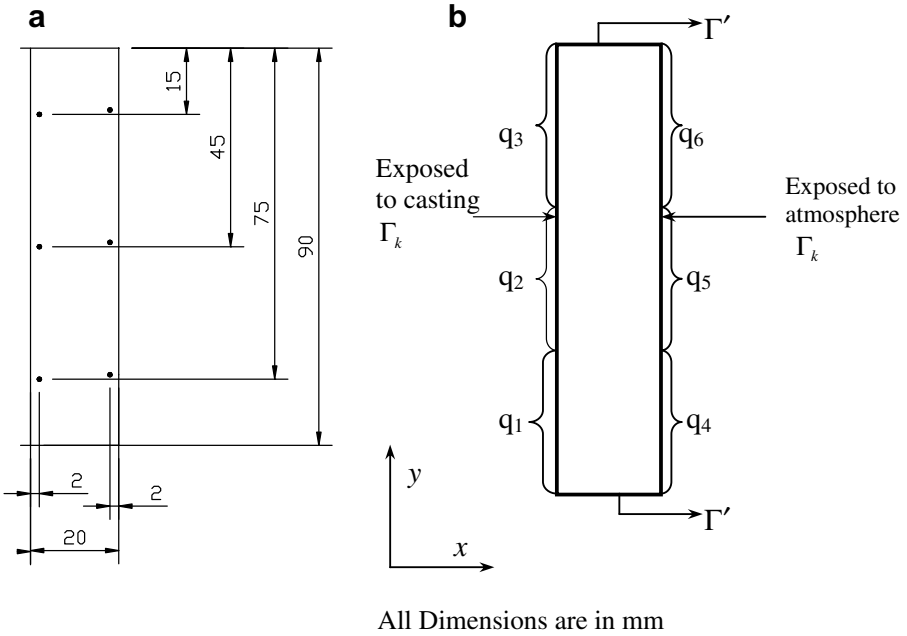

Fig. 2. Solution domain (mold wall). (a) Thermocouple locations and dimension of the mold and (b) boundary conditions.

tom, only the cast iron mold wall was considered as the solution domain (Fig. 2) for Serial-IHCP-algorithm. Both casting side and atmospheric side of the mold surfaces are considered as unknown boundaries and divided into six segments. The heat fluxes q_1–q_3 correspond to the metal–mold interface and q_4–q_6 represent the heat flux at the outer surface of the mold wall. In general, only the metal–mold interface is considered as unknown boundary and the outer surface of the mold wall is assigned with a nominal heat transfer coefficient. However, in the present formulation, the outer surface of the mold wall was also considered as an unknown boundary in order to avoid the error caused by the assumption of a constant heat transfer coefficient. The thermophysical properties and initial condition of the mold are given in Table 1. The 2D solution domain given in Fig. 2 was discretized into four-node iso-parametric elements. The total number of elements used in this case was 1800 (20×90). The convergence limit was set to be 1×10^{-6}.

The equation that governs the two-dimensional transient heat conduction within the solution domain was written as

$$\frac{\partial}{\partial x}\left(\lambda\frac{\partial T}{\partial x}\right)+\frac{\partial}{\partial y}\left(\lambda\frac{\partial T}{\partial y}\right)=\rho C_p\frac{\partial T}{\partial t} \tag{1}$$

with initial condition $T(x,y)=T'$ at $t=0$ and boundary conditions

$$-\lambda\frac{\partial T}{\partial x}n_x-\lambda\frac{\partial T}{\partial y}n_y=q_k(x,y,t) \quad \text{on } \Gamma_k;\ k=1,2,\ldots,p\ldots,l$$
$$-\lambda\frac{\partial T}{\partial x}n_x-\lambda\frac{\partial T}{\partial y}n_y=0 \qquad \text{on } \Gamma'$$

Table 1
Thermophysical properties of mold material

Density (ρ)	7274 kg/m^3
Specific heat (c)	420 J/kg K
Thermal conductivity (λ)	46 W/m K

The unknown heat fluxes along the inner and outer surfaces of the mold are vectorized into $(q_k)_i$; $k=1,2,\ldots,p\ldots,l$ and $i=1,2,\ldots m\ldots,n$. Once vectorized, the heat fluxes are treated as constant over the small interval of time Δt. Similarly, the thermal histories obtained from experiments are also vectorized into $Y_{j(i)}$; $j=1,2,\ldots,s$ and $i=1,2,\ldots,n$. The Serial-IHCP-algorithm adopted follows the steps given below in order to estimate unknown independent heat fluxes from the temperature measurements.

The multiple heat flux components are calculated serially, one after another, for every time step. The solution procedure is initiated by assuming the flux vectors $(q_k)_i$, $k=1,2,\ldots,p\ldots,l$, $i=1,2,\ldots m-1$; and $k=1,2,\ldots,p-1$; $i=1,2,\ldots m$ as known entities. This assumption enables us to find the temperature distribution within the mold wall by solving Eq. (1) using direct formulation.

The objective now is to find the heat flux $(q_p)_m$, where p and m are the present segment and time step, respectively. The incremental flux value for updating the heat flux $(q_p)_m$ is then computed from the expression given below, which is derived from the objective function.

$$(\Delta q_k)_m=\frac{\sum_{j=1}^{s}\sum_{i=1}^{r}[Y_{j,m+r-1}-\widehat{T}_{j,k,m+r-1}]\phi_{j,k,i}}{\sum_{j=1}^{s}\sum_{i=1}^{r}\left(\phi_{j,k,i}\right)^2} \tag{2}$$

where the sensitivity coefficient is as follows.

$$\phi_{j,k,i} = \frac{\left(\widehat{T}^{+}_{j,k,i} - \widehat{T}_{j,k,i}\right)}{\Delta q_{k,i}} \tag{3}$$

The terms in the numerator can be represented by the following notation and are computed by solving direct heat conduction equation using finite element method.

$$\widehat{T}^{+}_{j,k,i} = T_{j,k,i}\left|\begin{array}{l}(q_k)_{m\ldots m+r-1} = (q_k)_{m-1}; k = 1\ldots.l; k \neq p; \\ (q_p)_{m\ldots m+r-1} = (1+\varepsilon)(q_p)'\end{array}\right. \tag{4}$$

$$\widehat{T}_{j,k,i} = T_{j,k,i}|_{(q_k)_{m\ldots m+r-1}=(q_k)_{m-1};k=1\ldots p\ldots l;} \tag{5}$$

The incremental heat flux obtained from Eq. (2) is used to update the heat flux of the present segment. The corrected heat flux is then used to solve Eq. (1) to find the temperature distribution within the mold wall. Using this new temperature distribution, the incremental heat flux for the same boundary segment is again computed. This procedure is repeated till the incremental value reaches a minimum. The remaining unknown flux components are computed in a similar manner.

4. Results and discussion

The spatial variation of the air gap formation is often assumed to be uniform along the metal–mold interface of the mold wall. However, in gravity die-casting, the temperature distribution in the metal and the mold varies spatially due to the mold filling effects. In this section, we show the spatial variation of air gap and heat flux at the metal–mold interface in castings, where mold filling is involved.

We first discuss the temperature variation in the mold and casting due to mold filling effects using experimental measurements. Numerical results obtained from the Serial-IHCP-algorithm are then used to explain how these variations influence the air gap formation and thus affect the heat transfer at the metal–mold interface. Further, the two-dimensional nature of heat transfer in the mold during entire period of phase change is illustrated using the thermal field of mold wall obtained at different time steps.

4.1. Experimental results

In this section, we discuss the experimental temperature measurements of casting and mold regions. The location of thermocouples in the casting and mold regions are shown in Fig. 1b. Fig. 3a shows the cooling curves obtained at different thermocouple locations T1, T2, and T3 inside the casting. Fig. 3b shows a part of Fig. 3a for the initial 100 s. This figure is used to illustrate the filling effects and solidification of the metal during the initial stages of experiment. Fig. 3b clearly shows that the liquid metal solidifies within initial 100 s of the experiment. Thus the

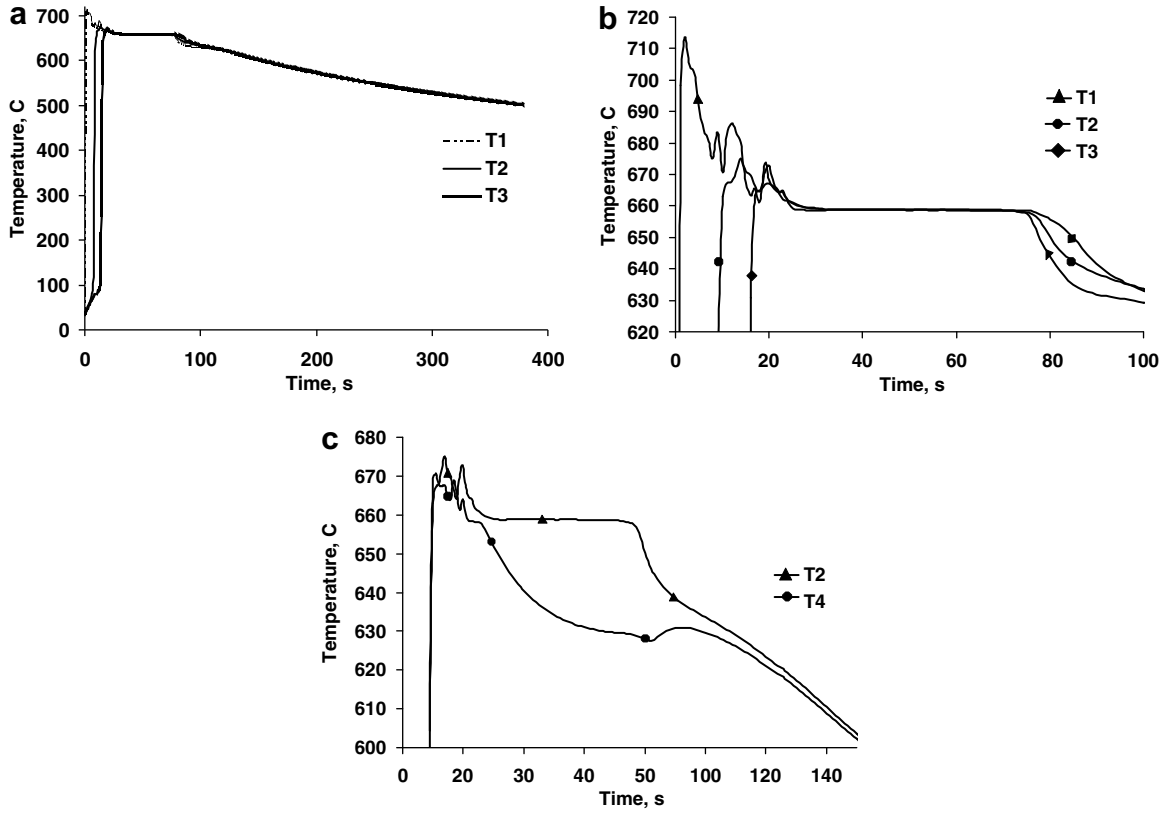

Fig. 3. (a) Time–temperature curve inside the casting, (b) time–temperature curve inside the casting for the initial 100 s and (c) temperature measurements at the horizontal mid plane.

measurements made during this time period is vital. In the casting experiment, the molten metal was filled from the bottom to the top. Since, the molten metal looses superheat during filling, the initial temperature decreases from the bottom (T1) to the top (T3), which is evident from Fig. 3b and Table 2. Consequently, the start and end time of solidification also varies at each thermocouple location. Fig. 3c shows the cooling curve of casting obtained at locations near and away from the mold wall in the horizontal mid section of the casting. This figure clearly shows the difference in solidification time between these two locations. The hot metal that comes in contact with the mold wall immediately looses its superheat and starts solidifying when compared to the metal away from the mold wall. As soon as the metal starts solidifying near the mold wall, an air gap begins to develop at the metal–mold interface due to the solidification shrinkage. This air gap affects the heat transfer at the metal–mold interface. Since the time at which the metal comes in contact with the mold wall varies from the bottom to top, the initiation of the air gap also varies along the vertical direction of the mold wall.

Table 2
Initial temperature, start and end of solidification at T1, T2 and T3

Thermocouple location	Initial temperature (C)	Starting time of solidification (s)	Ending time of solidification (s)
T1	713.77	27	68
T2	675.27	32	71
T3	667.06	35	75

Fig. 4a–c shows the temperature measurements obtained from the mold wall. The spatial variation of the temperature along the vertical direction is evident from Fig. 4a. The temperature difference is higher in the initial 150 s and it reduces as time progresses. The time–temperature curves are different from each other. The thermal shock in the bottom and the middle segment of the mold wall is large due to the high superheat of the metal and low initial temperature of the mold. During the time of filling the metal gradually looses the super heat and the temperature of the mold wall increases. By the time the metal comes in contact with the top portion of the vertical wall, it would have lost most of its super heat and hence the thermal shock is much lower. The above statement is corroborated by the smoothness of the cooling curve corresponding to the top thermocouple (T7). Further, in Fig. 4b, the sudden change in slope in the curves corresponding to T5 and T7 during the time period of 20–40 s is shown to be associated with the sudden onset of the air gap formation in the bottom and top portion of the mold wall. Fig. 4c indicates the temperature measurements at the thermocouple locations T8, T9, and T10 near the outer surface of the mold wall.

Figs. 3 and 4 clearly prove the following facts: (a) In gravity die-casting, there exists a variation in the temperature distribution due to filling effects. (b) The molten metal

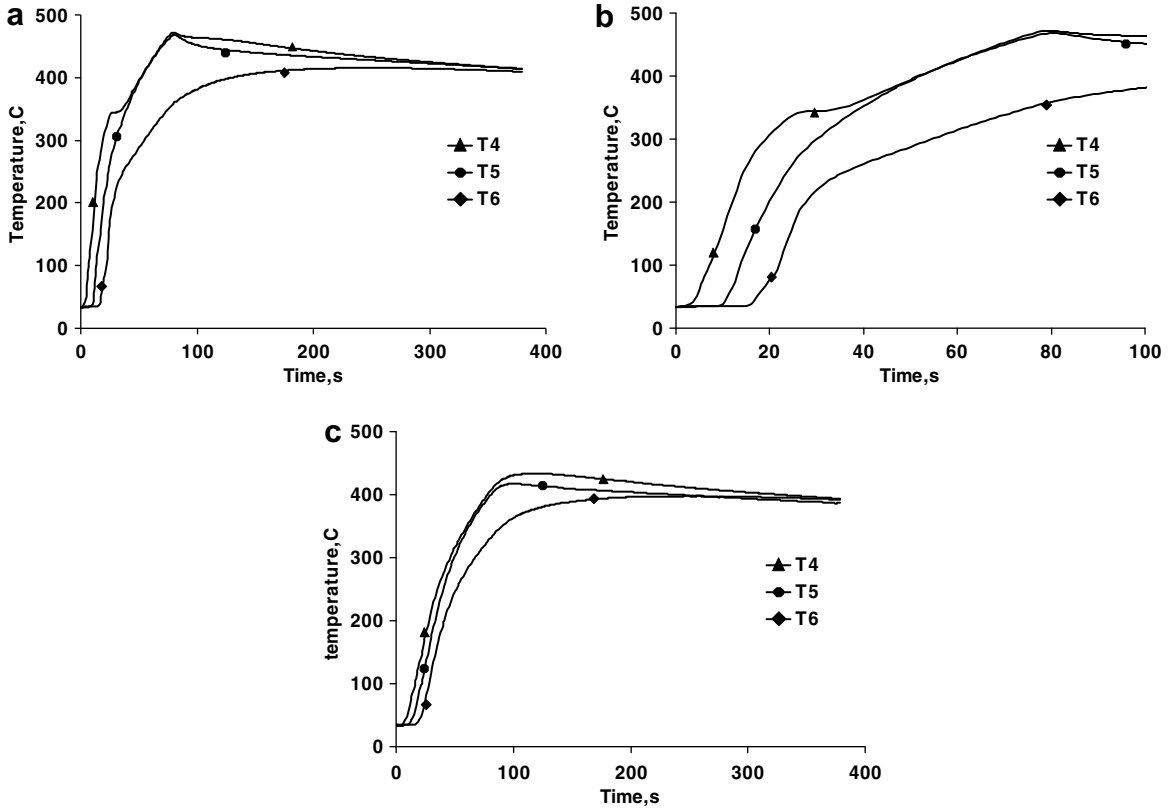

Fig. 4. Temperature measurements in the mold wall (a) near the metal–mold interface (b) for the initial 100 s (c) near the outer surface of the mold wall.

that comes in contact with the mold wall solidifies faster and forms a thin shell, which leads to a progressive development of air gap at the metal–mold interface. Since the time at which the molten metal comes in contact with the mold wall varies due to the filling effects, the formation of air gap also varies along the vertical mold wall.

4.2. Numerical results

The experimental temperature measurements were used to estimate the heat flux transients at the metal–mold interface using IHCP. Similar to all transient problems, the IHCP solution is also subject to numerical errors caused by large time steps. Therefore, we have chosen three different time steps ($\Delta t = 1$ s, 0.5 s, and 0.25 s) to analyze the results.

The absolute error between the estimated and measured temperatures at the thermocouple locations T5, T6, and T7 (near metal–mold interface) is given in Fig. 5a–c, respectively. These Figures clearly indicate that the error is higher at the early stages (0–50 s) and reduces as time progresses, irrespective of the time step Δt. These figures also show that the error between the measured and the predicted temperatures reduces as the time step Δt reduces. During initial time gap, the temperature variation with respect to time in the mold wall is higher. Hence, assigning larger time steps leads to error in the numerical predictions. It is evident from Fig. 5a–c that the error corresponding to time step $\Delta t = 0.25$ is negligible. Hence, the results obtained from the corresponding simulation are used in further discussions.

The mold wall exposed to the casing side is divided into three equal segments in order to estimate the heat flux at the metal–mold interface. The fluxes q_1–q_3 represent the heat flux at the bottom, middle and top segment of the metal–mold interface respectively. Fig. 6a and b shows the transient heat flux at the metal–mold interface and Fig. 6c shows the heat flux at the outer surface of the mold wall. The initial transient that is observed in the heat flux estimations in Fig. 6a is due to the mold filling effects. Due to the progressive filling of the liquid metal from bottom to top, instantaneous heating of the mold surface was practically not possible. Hence, the heat fluxes (q_1–q_3) reach the maximum after few seconds as opposed to the theoretical initial maximum (maximum heat flux at zero time). Fig. 6a clearly shows that the variation of the heat flux is high during initial stages. Beyond 100 s there is no significant variation in the heat flux distribution. Fig. 3b

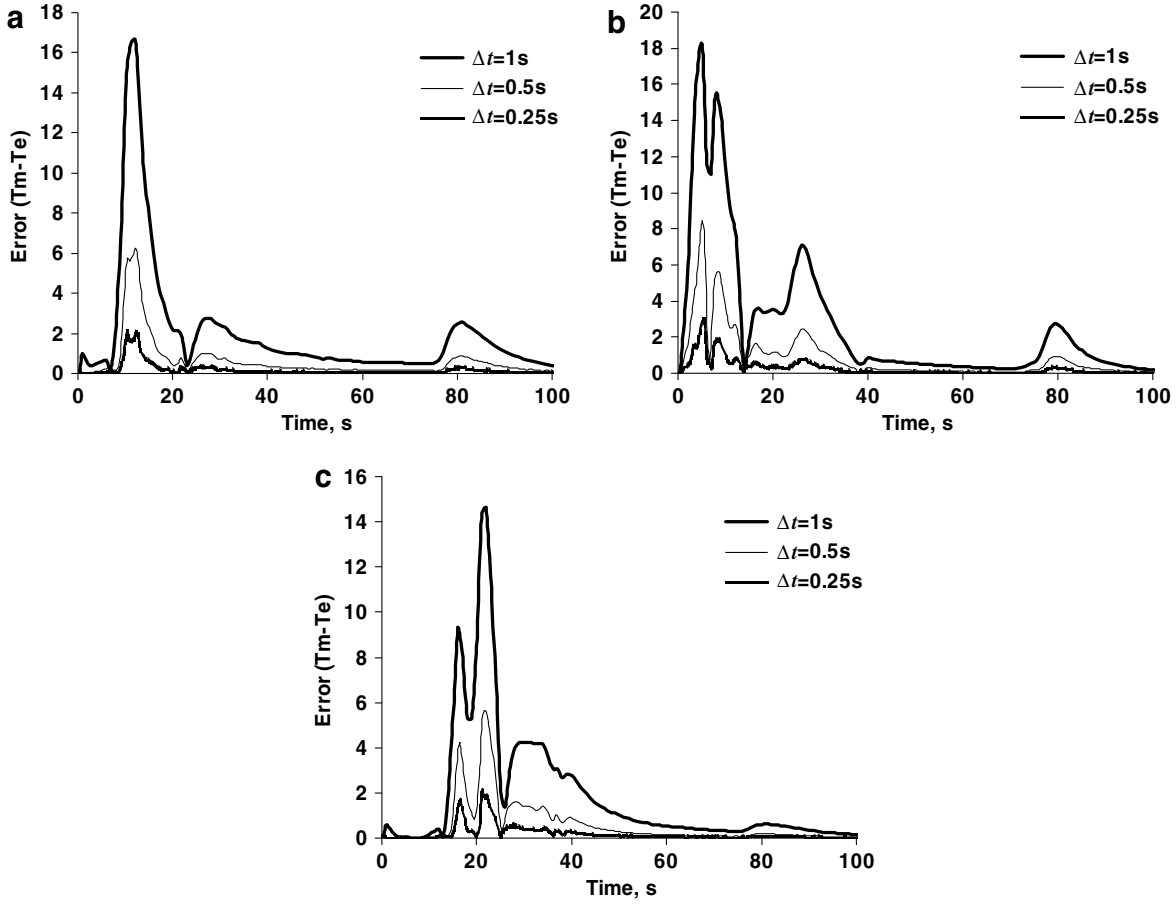

Fig. 5. Error between the predicted and measured temperature at various thermocouple locations: (a) thermocouple T5, (b) thermocouple T6, and (c) thermocouple T7.

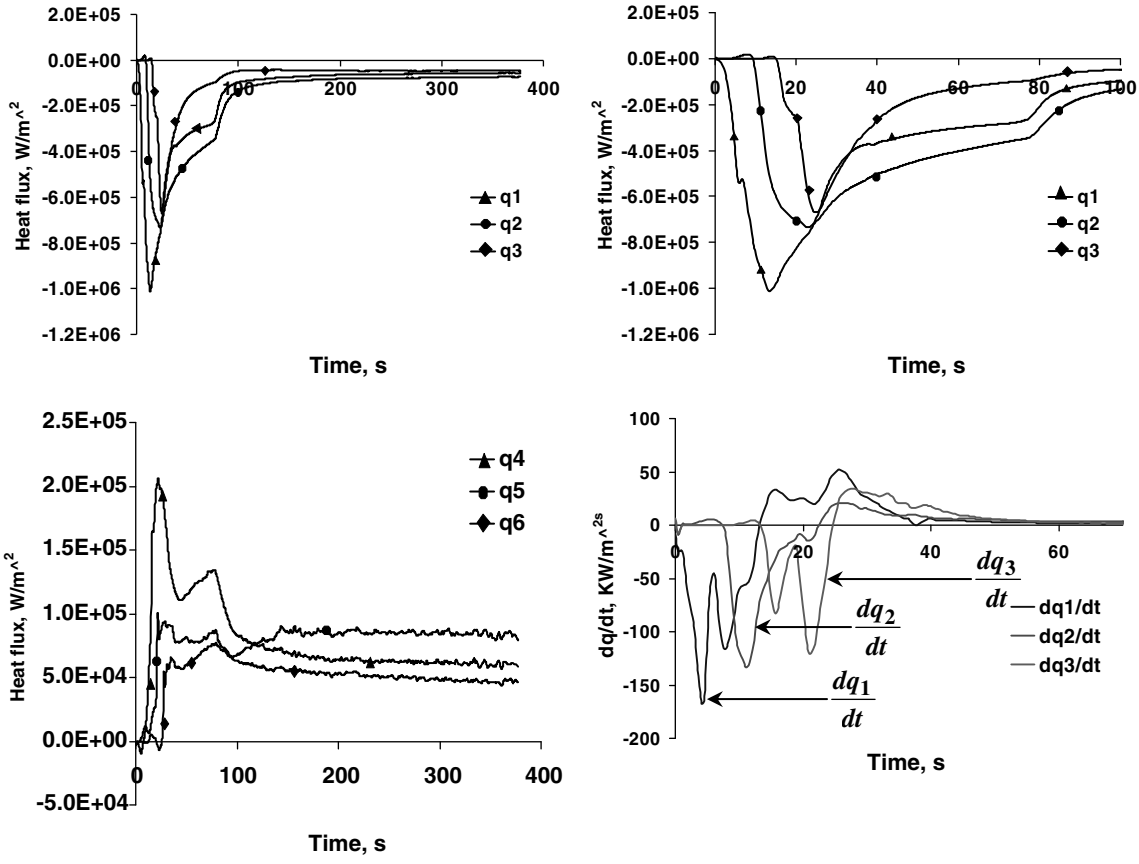

Fig. 6. Estimated flux components (a) flux at the metal–mold interface, (b) flux at the metal–mold interface for initial 100 s (c) flux at the outer surface of the mold wall and (d) rate of change of heat flux.

clearly shows that the solidification of the metal completes within the initial 100 s. Therefore, the flux distribution during the initial stages of solidification is more important than that at the later stages. The variation of heat flux in three different segments along the vertical mold wall for the initial 100 s is given in Fig. 6b. It is generally accepted that the air gap begins to form when the heat flux at the metal–mold interface reaches its peak value. The time at which the flux at each segment reaches the peak value is given in Table 3. Fig. 6b and Table 3 clearly indicate that the heat flux reaches the maximum value at different times in different segments. Therefore, the air gap initiation also differs for each segment of the metal–mold interface.

Fig. 6d shows the rate of change of heat flux with respect to time. This figure shows that the air gap formation first starts from the bottom of the cavity then in the middle and top. This can be corroborated with the sudden drop in heat flux during the time period of 10–30 s in the bottom segment (Fig. 6b). On the contrary, the heat flux at the middle segment decreases gradually. This shows that the air gap is comparatively smaller in the middle segment than the bottom. Since the liquid metal looses most of its superheat when it comes in contact with the top segment, the heat flux is low when compared to other two segments. Further, Fig. 6b shows that heat flux at the middle segment is more than that of the top and bottom during the period of phase change. This indicates that the air gap formation is less in the middle when compared to top and bottom of the mold wall.

Table 3
Maximum Heat Flux at the metal–mold interface and corresponding time

	Maximum heat flux (q_{max}) (KW/m^2)	Time (s)
q_1	1009.764	13.75
q_2	733.641	23
q_3	669.927	24.75

Fig. 7 shows the thermal field in the mold at different time steps. The thermal fields at the time steps t=10, 15, 25 s clearly indicate the gradual heating of the mold wall during filling. The heat transfer within the mold wall remain two-dimensional during the entire period of phase change (up to 100 s), which is clearly evident from the Fig. 7. The initial variation in the thermal field is caused by the filling transients and further enhanced by the spatial variation of the heat flux at the metal–mold interface. The heat transfer becomes almost one dimensional at 350 s.

The results obtained from Serial-IHCP-algorithm bring out the following facts: (a) The heat flux at the metal–mold interface reaches peak values at different times along different segments of the mold wall. This shows that the initiation of air gap formation is different along the metal–mold interface. (b) The air gap formation is first initiated

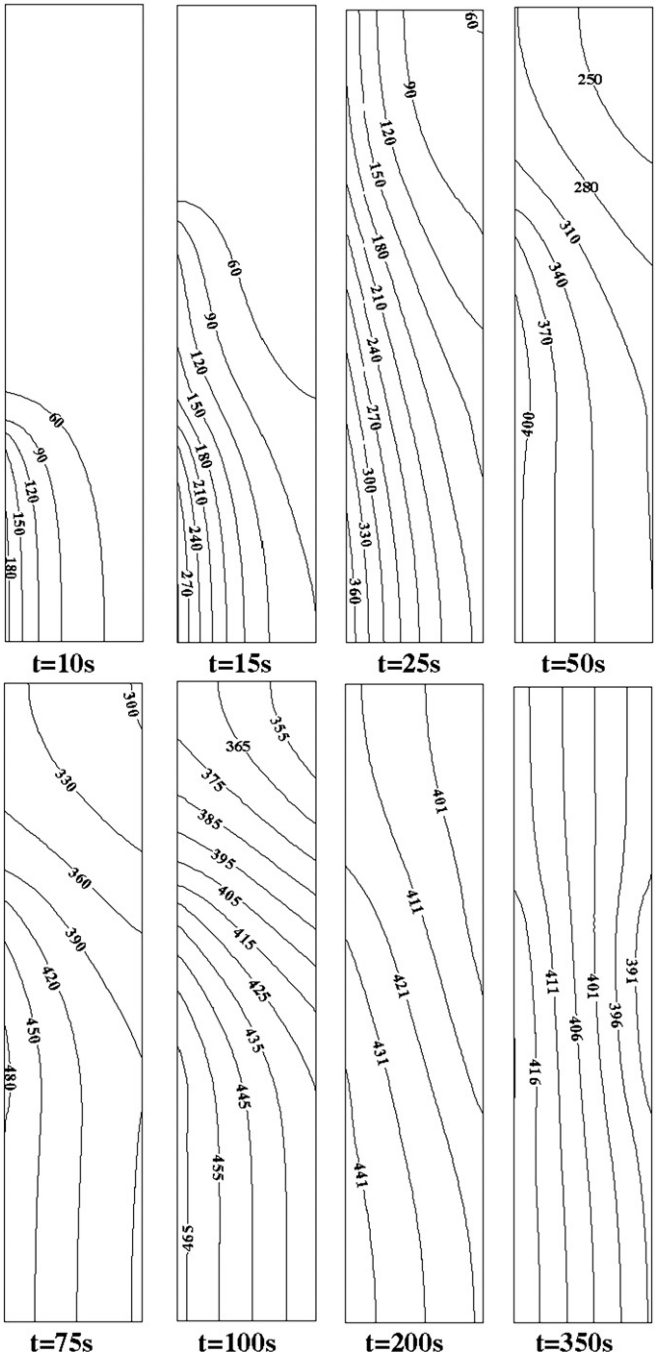

Fig. 7. Thermal field in the mold wall for various time steps.

in the bottom and then in the middle and top of the vertical wall. (c) The heat flux at the metal–mold interface during phase change is more in the middle than the bottom and top. This shows that the air gap is minimum at the middle. (d) The heat transfer in the mold wall is two-dimensional during the entire period of the phase change.

5. Conclusion

Most of the research work in solidification either assumes no spatial variation in the air gap formation or limits their study to those experimental systems in which air gap formation is uniform. However, in gravity die-casting, filling effects creates variation in thermal field in the mold and casting regions. This paper shows that this variation greatly influences the time of air gap initiation along a vertical mold wall. This subsequently leads to the spatial variation of air gap and in turn the heat flux at the metal–mold interface.

In order to study the spatial variation of interface heat flux, an experimental setup that involved mold filling was devised. Commercially available aluminum of 99.9% purity was used as a casting material and cast-iron was used as mold wall material. The Serial-IHCP-algorithm was used to estimate the multiple heat flux transients along the metal–mold interface. The major observations made in this paper pertaining to experimental and numerical investigations are summarized below.

(a) The temperature measurements at the casting and mold regions show that the time at which the molten metal comes in contact with the mold wall differs along the vertical direction due to mold filling.
(b) The heat flux at the metal–mold interface reaches peak values at different times along different segments of the mold wall. This shows that the initiation of air gap formation varies along the metal–mold interface.
(c) The air gap formation is first initiated at the bottom, middle, and then at the top of the vertical wall.
(d) During phase change, the heat flux at the mid segment of the metal–mold interface was found to be higher than the bottom and top segments under the experimental conditions. This shows that the air gap was minimum at the middle.
(e) From the above conclusions, it is anticipated that the complex nature of heat transfer that exists during the entire period of phase change at the metal–mold interface could influence the convection in the mushy region in the case of alloy solidification. In such cases, it is important to consider the spatial variation of air gap due to filling transients, in addition to geometrical factors, and its effect on the heat transfer at the metal–mold interface.

References

[1] O. Richmond, R.H. Tien, Theory of thermal stress and air-gap formation during the early stages of solidification in a rectangular mold, J. Mech. Phys. Solids. 19 (1971) 273–284.
[2] Y. Nishida, W. Droste, S. Engler, The air gap formation process at the casting-mold interface and the heat transfer mechanism through the gap, Metall. Mater. Trans. B 17B (1986) 833–844.
[3] T.S. Prasanna Kumar, K. Narayan Prabhu, Heat flux transients at the casting/chill interface during solidification of aluminum base alloys, Metall. Mater. Trans. B 22B (1991) 717–727.
[4] F. Michel, P.R. Louchez, F.H. Samuel, Heat transfer coefficient during solidification of Al–Si alloys: effects of mold temperature, coating type and thickness, AFS Trans. 9 (1995) 275–283.

[5] K. Narayan Prabhu, John Campbell, investigation of casting/chill interfacial heat transfer during solidification of Al–11% Si alloy by inverse modeling and real-time X-ray imaging, Int. J. Cast Metal Res. 12 (1999) 137–143.
[6] W.D. Griffiths, Modeled heat transfer coefficients for Al–7 wt-%Si alloy castings unidirectionaly solidified horizontally and vertically downwards, Mater. Sci. Technol. 16 (2000) 255–260.
[7] M.A. Martorano, J.D.T. Capocchi, Heat transfer coefficient at the metal–mould interface in the unidirectional solidification of Cu–8%Sn alloys, Int. J. Heat Mass Transfer 43 (2000) 2541–2552.
[8] P.A. Kobryn, S.L. Semiatin, Determination of interface heat-transfer coefficients for permanent-mold casting of Ti–6Al–4V, Metall. Mater. Trans. B 32B (2001) 685–695.
[9] Kai Ho, Robert D. Pehlke, Metal/mold interface heat transfer, Metall. Mater. Trans. B 16B (1985) 585–594.
[10] Michael Trovant, Stavros Argyropoulos, Finding boundary conditions: a coupling strategy for the modeling of metal masting processes: Part I. Experimental study and correlation development, Metall. Mater. Trans. B 31B (2000) 75–86.
[11] Michael Trovant, Stavros Argyropoulos, Finding boundary conditions: a coupling strategy for the modeling of metal casting processes: Part II. Numerical Analysis, Metall. Mater. Trans. B 31B (2000) 87–96.
[12] Carlos A. Santos, Claudio A. Siqueira, Amauri Garcia, Jose M.V. Quaresma, Jaime A. Spim, Metal–mold heat transfer coefficients during horizontal and vertical unsteady solidification of Al–Cu and Sn–Pb alloys, Inverse Probl. Sci. Eng. 12 (2004) 279–296.
[13] T. Loulou, E.A. Artyukhin, J.P. Bardon, Estimation of thermal contact resistance during the first stages of solidification process: I – Experiment principle and modelisation, Int. J. Heat Mass Transfer 42 (1999) 2119–2127.
[14] T. Loulou, E.A. Artyukhin, J.P. Bardon, Estimation of thermal contact resistance during the first stages of solidification process: II – Experimental setup and results, Int. J. Heat Mass Transfer 42 (1999) 2129–2142.
[15] K. Narayana Prabhu, K.M. Suresha, Effect of superheat, mold, and casting materials on the metal/mold interfacial heat transfer during solidification in graphite-lined permanent molds, J. Mater. Eng. Perform. 13 (2004) 619–626.
[16] C.P. Hallam, W.D. Griffiths, A Model of the interfacial heat-transfer coefficient for the aluminum gravity die-casting process, Metall. Mater. Trans. B 35B (2004) 721–733.
[17] T.S. Prasanna Kumar, H.C. Kamath, Estimation of multiple heat flux components at the metal/mould interface in bar and plate aluminum alloy castings, Metall. Mater. Trans. B 35B (2004) 575–585.
[18] J. Majumdar, B.C. Raychauduri, S. Dasgupta, An instrument scheme for multipoint measurement of mold-metal gap in an ingot casting system, Int. J. Heat Mass Transfer 24 (1981) 1089–1095.
[19] H.K. Kim, S.I. Oh, Evaluation of heat transfer coefficient during heat treatment by inverse analysis, J. Mater. Process. Technol. 112 (2001) 157–165.
[20] J.V. Beck, Inverse problems in heat transfer with application to solidification and welding, Model. Cast. Weld. Adv. Solid. V (1991) 503–514.
[21] A.A. Tseng, F.Z. Zhao, Multidimensional inverse transient heat conduction problems by direct sensitivity coefficient method using a finite element scheme, Numer. Heat Transfer Part B 29 (2000) 365–380.
[22] T.S. Prasanna Kumar, A serial solution for the 2-D inverse heat conduction problem for estimating multiple heat flux components, Numer. Heat Transfer Part B 45 (2004) 541–563.